


ORIGINAL ARTICLE

Promotion of tumorigenesis by miR-1260b–targeting CASP8: Potential diagnostic and prognostic marker for breast cancer

Sunyoung Park^{1,2} | Jungho Kim^{1,3} | Yoonjung Cho^{1,4} | Sungwoo Ahn¹ |
 Geehyuk Kim^{1,5} | Dasom Hwang¹ | Yunhee Chang¹ | Sunmok Ha¹ | Yeonim Choi⁶ |
 Min Ho Lee^{1,4} | Hyunju Han⁷ | Sunghyun Kim³ | Seung Il Kim⁷  | Hyeyoung Lee¹

¹Department of Biomedical Laboratory Science, College of Health Sciences, Yonsei University, Wonju, Korea

²School of Mechanical Engineering, Yonsei University, Seoul, Korea

³Department of Clinical Laboratory Science, College of Health Sciences, Catholic University of Pusan, Busan, Korea

⁴Forensic DNA Division, National Forensic Service, Wonju, Korea

⁵Division of Public Health Emergency & Bioterrorism, Centers for Disease Control & Prevention, Cheongju, Korea

⁶Department of Biomedical Laboratory Science, Songho College, Hoengseong, Korea

⁷Department of Surgery, College of Medicine, Yonsei University, Seoul, Korea

Correspondence

Seung Il Kim, Department of Surgery, Yonsei University College of Medicine, 50 Yonsei-Ro, Seodaemun-Gu, Seoul 120-752, Korea.

Email: skim@yuhs.ac

Hyeyoung Lee, Department of Biomedical Laboratory Science, College of Health Sciences, Yonsei University, 1 Yonsei-dae-gil, Wonju-si, Gangwon-do 26493, Korea.
 Email: hylee@yonsei.ac.kr

Abstract

MicroRNAs are reported as promising biomarkers for the diagnosis and treatment of breast cancer. miR-1260b is identified as a tumor-associated noncoding microRNA in other cancers, although the role of miR-1260b and its clinical relevance in breast cancer remain unclear. In this study, miR-1260b as a potential prognostic biomarker was observed by univariate and multivariate Cox regression analyses in 102 breast tumor tissues. The tumorigenic role of miR-1260b in terms of proliferation, apoptosis, and migration of breast cancer cells was investigated using gain- and loss-of-function assays in vitro. Additionally, the potential early diagnosis and treatment monitoring marker of miR-1260b was validated in 129 plasma samples. We found that high miR-1260b expression was markedly associated with bulky tumor size, advanced stage, and lymph node invasion. Particularly, the high-miR-1260b-expression group showed shorter overall survival than the low-miR-1260b-expression group. The inhibition of oncogenic miR-1260b induced apoptosis and decreased migration and invasion of MDA-MB-231 cells. CASP8 was revealed as a direct target gene of miR-1260b, which is closely related to apoptosis. Furthermore, miR-1260b expression levels in plasma were significantly higher in patients with breast cancer than in healthy controls. The patients who tested positive for miR-1260b showed 16.3- and 18.2-fold higher risks in the early stage and locally advanced stage, respectively, compared with healthy controls, and the risk was decreased 6.2-fold after neoadjuvant chemotherapy. Taken together, miR-1260b may be a potential novel diagnostic, prognostic, and therapeutic target in breast cancer.

[Correction added on 6 June 2022, after first online publication: The gene name was corrected from "CAPS8" to "CASP8" on the Title, Materials and Methods, Results, Discussion and Figure 3.]

Abbreviations: ATCC, American Type Culture Collection; AUC, area under the receiver-operating characteristic curve; CA15-3, carbohydrate antigen 15-3; CEA, carcinoembryonic antigen; DEG, differentially expressed gene; DMEM, Dulbecco's modified Eagle's medium; ER, estrogen receptor; FBS, fetal bovine serum; FDR, false discovery rate; FFPE, formalin-fixed, paraffin-embedded; GO, gene ontology; HER2, human epidermal growth factor receptor type2; miRNAs, microRNAs; OS, overall survival; PI, propidium iodide; PR, progesterone receptor; PTPRK, tyrosine phosphatase receptor type kappa; RPMI, Roswell Park Memorial Institute; RT, reverse transcriptase; SFRP1, secreted frizzled-related protein 1; TCGA, The Cancer Genome Atlas; TNBC, triple-negative breast cancer; UTRs, untranslated regions.

Sunyoung Park and Jungho Kim contributed equally to this work.

Clinical Trial Registration Information: Written informed consent was obtained from all participants. The study was approved by the Institutional Ethics Committee of Yonsei Severance Hospital (approval no. 4-2016-0550, 4-2011-0011) and Yonsei University Wonju College of Medicine (approval no. 1041849-201603-BR-010-04).

This is an open access article under the terms of the [Creative Commons Attribution-NonCommercial](https://creativecommons.org/licenses/by-nc/4.0/) License, which permits use, distribution and reproduction in any medium, provided the original work is properly cited and is not used for commercial purposes.

© 2022 The Authors. *Cancer Science* published by John Wiley & Sons Australia, Ltd on behalf of Japanese Cancer Association.

Funding information

National Research Foundation of Korea, Grant/Award Number: NRF-2020R111A1A01067448

KEYWORDS

breast cancer, CASP8, diagnosis, miR-1260b, prognosis

1 | INTRODUCTION

Breast cancer is the most common malignancy in women, with nearly 2.1 million incidences worldwide annually. Breast cancer accounts for approximately 25% of all cancer cases and 15% of all deaths in women.^{1,2} Approximately 90% of breast cancer deaths have been attributed to metastasis-related complications.³

Despite the commitment to research on biomarkers for diagnosis, prognosis, and therapeutic response in breast cancer in the last decade, there are still many difficulties in the management of breast cancer. Mammography for breast cancer is currently a widely used screening tool; however, the extensive use of mammography has been hindered by the cost and expertise needed for mammography. Contrastingly, alternative methods, such as ultrasound screening are highly operator dependent. Additionally, tumor serum markers, such as carbohydrate antigen 15-3 (CA15-3) and carcinoembryonic antigen (CEA) are nonspecific and limited in their sensitivity and specificity.⁴⁻⁹ Therefore, it is necessary to develop a cost-effective and accurate test method for breast cancer by uncovering a new mechanism for breast cancer development.

Numerous studies reported that microRNAs (miRs or miRNAs) involved in various biological processes are potential diagnostic, prognostic, and therapeutic target biomarkers in many different types of cancer.¹⁰ miRNAs are small (18-25 nucleotides) endogenous noncoding RNAs that bind to the 3-untranslated regions (UTRs) of target mRNAs and inhibit translation or induce sequence-specific degradation of mRNAs, thereby silencing gene expression.¹¹ miRNAs have emerged as a key component of cancer biology by modulating the expression of their target mRNAs, promoting tumor growth, invasion, angiogenesis, metastasis, and immune evasion.^{12,13} The important role of miRNAs in tumorigenesis can provide new opportunities for cancer diagnosis and prognosis prediction.

miR-1260b mapped to human 11q21 was first identified in human renal cancers using a microRNA microarray.¹⁴ A recent study showed that the high expression level of miR-1260b in patients with colorectal cancer was associated with lymph node metastasis and invasion of the veins.¹⁵ miR-1260b, which is also highly expressed in prostate cell carcinoma tissues, promotes cell migration and invasion in prostate cancer cells by targeting secreted frizzled-related protein 1 (SFRP1) and SMAD4.¹⁶ Furthermore, miR-1260b promotes the migration and invasion of non-small cell lung cancer by targeting protein tyrosine phosphatase receptor type kappa (PTPRK).¹⁷ Comprehensive analysis showed that miR-1260b was highly expressed in the breast cancer cell MDA-MB-231-derived exosomes, compared with that in the normal breast cell MCF-10A-derived exosomes.¹⁸ However, the potential diagnostic or prognostic value of miR-1260b in clinical settings has not been fully investigated. Furthermore, the molecular mechanisms of miR-1260b in breast cancer tumorigenesis remain unknown. In

the present study, we evaluated the potential of miR-1260b as a biomarker for the diagnosis and prognosis of breast cancer and investigated its biological functions in the tumorigenesis of human breast cancer cells.

2 | MATERIALS AND METHODS

Detailed information is provided in [Supporting Information](#).

2.1 | Study population

A total of 102 formalin-fixed, paraffin-embedded (FFPE) breast tissue samples were obtained from patients with breast cancer at Yonsei Severance Hospital, Seoul, Republic of Korea, from 2010 to 2015 (Table S1). The study was approved by the Institutional Ethics Committee of Yonsei Severance Hospital (approval no. 4-2016-0550).

A total of 71 blood samples were obtained from patients with breast cancer at Yonsei Severance Hospital, Seoul, Republic of Korea from 2010 to 2015. For healthy controls, 58 blood samples were obtained from healthy donors (Table S2). The study was approved by the Institutional Ethics Committee at Yonsei Severance Hospital (approval no. 4-2011-0011) and Yonsei University Wonju College of Medicine (approval no. 1041849-201603-BR-010-04). Written informed consent was obtained from all participants.

2.2 | RNA extraction of FFPE tissues and plasma samples

Three to four 10- μ m thick sections of FFPE breast tissue were used for total RNA extraction. To remove paraffin from FFPE tissues, 160 μ l of deparaffinization solution (Qiagen) was added and vortexed, which was followed by incubation for 3 minutes at 56°C. RNA extraction was performed using the Qiagen RNeasy FFPE kit (Qiagen) according to the manufacturer's protocol, and 25 μ l of RNA was eluted.

For the extraction of miRNA from the plasma, a NucleoSpin miRNA Plasma kit (Macherey-Nagel) was used according to the manufacturer's protocol. The purity and concentration of total RNA were determined by measuring the ratio of absorbance values at 260 and 280 nm using a spectrophotometer. Isolated RNA was stored at -80°C until use.

2.3 | microRNA reverse-transcriptase quantitative (RT-qPCR) analysis

The following TaqMan small RNA assays (Applied Biosystems by Life Technologies) were used: RNU6B, hsa-miR-16, and hsa-miR-1260b.

Reverse-transcriptase qPCR reactions were performed on a CFX96 real-time PCR system detector (Bio-Rad). Samples were run in duplicate for each experiment. Data were analyzed using the comparative ΔC_T ($2^{-\Delta C_T}$) and $\Delta\Delta C_T$ methods ($2^{-\Delta\Delta C_T}$) with miR-16 for plasma or RNU6B for cell lines and tissues as an endogenous control.^{19,20} To monitor reagent contamination, a negative control was included for each primer pair.

2.4 | Cell culture

Human breast normal cells (MCF-10A) and breast cancer cell lines (MCF-7, BT-474 SKBR-3, and MDA-MB-231) were purchased from the American Type Culture Collection (ATCC). MCF-10A cells were cultured in mammary epithelial cell basal medium (MEBM) supplemented with mammary epithelial cell growth medium (MEGM) Single Quots and cholera toxin (Lonza). SKBR-3 and MDA-MB-231 cells were cultured in Roswell Park Memorial Institute (RPMI)-1640 (Gibco) supplemented with 10% fetal bovine serum (FBS; Gibco) and 100 units/ml of streptomycin-penicillin (Gibco). MCF-7 and BT-474 cells were cultured in Dulbecco's modified Eagle's medium (DMEM; Gibco) supplemented with 10% FBS and 100 units/ml of streptomycin-penicillin. All cells were incubated at 37°C in a 5% CO₂ atmosphere.

2.5 | Cell apoptosis analysis

Annexin V and propidium iodide (PI) staining was performed using the Annexin V-FITC Apoptosis Detection Kit 1 (BD Biosciences) according to the manufacturer's instructions. Cell apoptosis was analyzed using a BD FACS Calibur flow cytometer (BD Biosciences) and FlowJo (TreeStar Inc.).

2.6 | Wound-healing and transwell invasion assays

Cell migration assays were performed using SPLScar™ (SPL) according to the manufacturer's instructions. The wound-healing images and wound closure were analyzed using a light microscope (CKX41, Olympus) and the ImageJ program (National Institutes of Health, Bethesda, MD, USA) at 0, 12, and 24 hours.

Cell invasion assays were performed using SPLInsert™ Hanging (8 μm, SPL) according to the manufacturer's instructions. The chambers were inserted into 24-well plates, and transfected cells (5×10^4 cells) were seeded in the upper chambers. Medium containing 0.1% FBS was added to the upper chambers, while medium containing 20% FBS was added to the lower chamber. The cells were then incubated for 48 hours at 37°C and 5% CO₂. After incubation, the membrane was trimmed, stained with 0.1% crystal violet, and observed under a light microscope. Three fields were randomly selected from each membrane, and the number of invaded cells was counted.

2.7 | Western blot analysis

Cell lysates treated identically were pooled and centrifuged at 13,000 g at 4°C for 10 minutes. The supernatants were subjected to Western blot analysis, as described in the [Supporting Information](#). Total cell protein (15–20 μg) was used for Western blotting (Table S3).

2.8 | RNA sequence analysis

The concentration and quality of total RNA were checked using a Qubit 2.0 fluorometer (Thermo Fisher Scientific). Total RNA (10 ng) was used to prepare strand-specific barcoded RNA libraries using the Ion AmpliSeq™ Transcriptome Human Gene Expression Kit (Thermo Fisher Scientific) following the manufacturer's protocol.

2.9 | Luciferase assay

Plasmids were constructed using the pmirGLO Dual-Luciferase miRNA Target Expression Vector (Promega) for the binding site in the 3'-UTR of the mRNA of the potential target gene (*CASP8*) based on TargetScan 7.2 (Bioneer Service System, Bioneer). The sequences of *CASP8* wild type (WT) and mutant type (MT) are described in Table S4. For the reported gene assay, MDA-MB-231 cells were cotransfected with reporter vectors (*CASP8* WT or *CASP8* MT), the miR-1260b mimic, and the negative control. Luciferase and Renilla signals were measured 24 hours after transfection using the Dual-Luciferase Reporter Assay System (Promega).

2.10 | Statistical analysis

Statistical analysis was performed using GraphPad Prism software (version 6.0) and SPSS Statistics software (version 21.0; IBM). Values with $p < 0.05$ were considered statistically significant in all the analyses.

3 | RESULTS

3.1 | Association of high miR-1260b expression with aggressive clinicopathological features and poor prognosis in breast cancer

To explore the relationship between clinicopathological characteristics and miR-1260b expression, the expression levels of miR-1260b in 102 breast cancer FFPE tissues were measured using RT-qPCR (Table S1). The patients were divided into low- and high-miR-1260b-expression groups based on the median miR-1260b expression level (low-expression group, <2.54 ; high-expression group, ≥ 2.54).

(Figure 1A). The association between the expression of miR-1260b and overall survival (OS) was investigated using Kaplan-Meier analysis and the log-rank test. High expression of miR-1260b resulted in a poor survival outcome (hazard ratio [HR] = 13.51 (3.30-15.92), $p < 0.0001$) (Figure 1B).

The potential relationship between clinicopathological parameters, such as age, TNM (tumor [T], node [N], and metastasis [M]) stage, histological grade, tumor size, lymph node invasion, human epidermal growth factor receptor type2 (HER2), estrogen receptor (ER), progesterone receptor (PR), and the expression levels of miR-1260b were analyzed using the chi-square test. The results showed that locally advanced stage ($p < 0.01$), larger tumors ($p < 0.001$), and presence of lymph node invasion ($p < 0.05$) were significantly associated with high miR-1260b expression levels (Table 1). Furthermore, the expression levels of miR-1260b were significantly increased in the locally advanced and metastatic stages compared with those in the early stage ($p < 0.01$, $p < 0.001$, respectively) (Figure 1C).

To analyze the prognostic parameters of miR-1260b, Cox proportional hazards regression was used to investigate the association between the survival time of patients and the clinical parameters of miR-1260b expression. Univariate analysis showed that high miR-1260b (HR = 8.52, $p < 0.01$), locally advanced stage (HR = 9.02, $p < 0.001$), larger tumor size (HR = 5.62, $p < 0.01$), presence of lymph node invasion (HR = 4.28, $p < 0.05$), HER2 positivity (HR = 4.71, $p < 0.05$), and ER negativity (HR = 0.35, $p < 0.05$) were associated with poor prognosis in patients with breast cancer. All significant parameters were further analyzed using a multivariate analysis. The results showed that TNM stage (HR = 6.05, $p < 0.01$), tumor size (HR = 5.72, $p < 0.01$), lymph node invasion (HR = 3.60, $p < 0.05$), HER2 (HR = 3.77, $p < 0.01$), ER (HR = 0.31, $p < 0.05$), and miR-1260b (HR = 5.11, $p < 0.05$) were independent prognostic factors for patients with breast cancer (Table 2). Furthermore, patients with high miR-1260b expression in the

early stage, locally advanced stage, and metastatic stage indicated a high risk of poor prognosis (HR = 5.77, 3.82, and 4.22) (Figure 1D).

To cross-validate the prognostic value of miR-1260b, The Cancer Genome Atlas (TCGA) data of breast cancer including molecular subtypes was utilized. Consistent with our results, high miR-1260b expression was associated with worse survival (HR = 1.74) (Figure S1). Specifically, high miR-1260b expression in patients with the luminal A and triple-negative breast cancer (TNBC) subtypes showed relatively poor survival outcomes (HR = 5.85, $p = 0.007$; HR = 3.58, $p = 0.022$, respectively) (Figure S1G-J).

3.2 | Promotion of migration and invasion in metastatic breast cancer cell by miR-1260b

To investigate how miR-1260b modulates the status of breast cancer, the levels of miR-1260b in four representative breast cancer cell lines (BT-474, MCF-7, SKBR-3, and MDA-MB-231) and a normal breast cancer cell line (MCF-10A) were screened to identify a representative in vitro model. The MDA-MB-231 cell line, which is a representative cell line of aggressive and metastatic breast cancer showed higher expression of miR-1260b compared with both normal breast cancer cell line (MCF-10A) and less aggressive breast cancer cell line (MCF-7) (Figure 2A).

Therefore, we selected MDA-MB-231 cells for the transfection experiments. miR-1260b was well transfected into the cells. Specifically, the cells treated with the miR-1260b mimic showed overexpression of miR-1260b, whereas cells treated with the miR-1260b inhibitor showed effective suppression of miR-1260b expression ($p < 0.01$ and $p < 0.01$, respectively) (Figure 2B). The proliferative effect of miR-1260b expression significantly increased upon transfection with the miR-1260b mimic and decreased markedly upon the

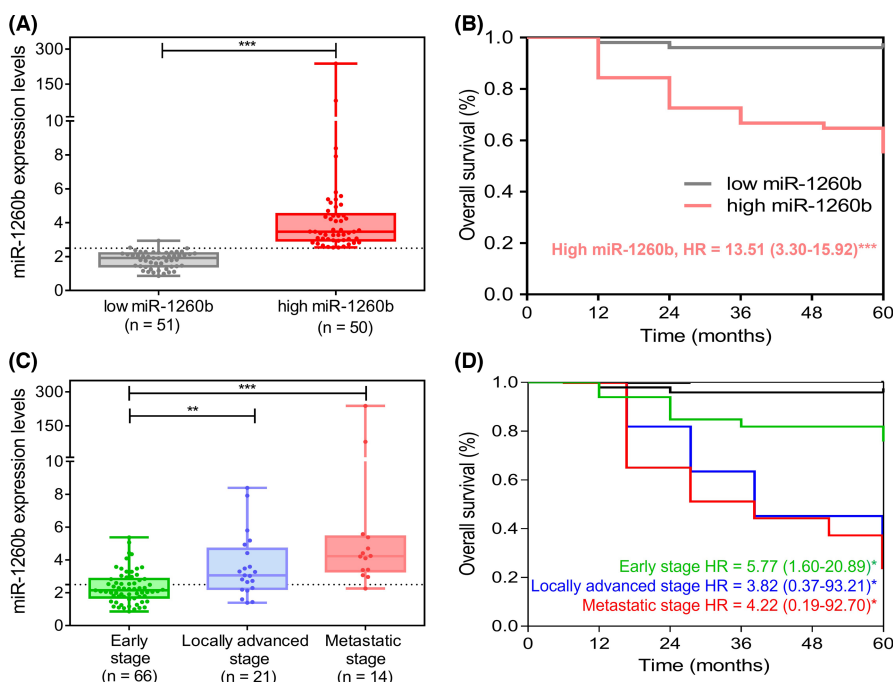


FIGURE 1 Graphs depicting the prognostic value of miR-1260b in breast cancer. A, The expression levels of low and high miR-1260b in FFPE breast tissues of breast cancer. B, Kaplan-Meier survival for low miR-1260b expression level versus high miR-1260b expression level in breast cancer. C, The expression levels of miR-1260b in FFPE breast tissues according to early-stage, locally advanced, and metastatic breast cancer. D, Kaplan-Meier survival for low miR-1260b expression level versus high miR-1260b expression level in early-stage, locally advanced, and metastatic breast cancer. The data are reported as the mean \pm standard deviation (SD). * $p < 0.05$, ** $p < 0.01$, *** $p < 0.001$

TABLE 1 Association of miR-1260b expression with clinicopathological parameters in breast cancer patients

Variable	n	miR-1260b expression		P value
		Low, n (%)	High, n (%)	
Age (years)				
<50	54	30 (55.6)	24 (44.4)	0.172
≥50	48	20 (41.7)	28 (58.3)	
TNM stage				
I/II (early stage)	70	45 (64.3)	25 (35.7)	<0.01
III (locally advanced stage)	17	4 (17.6)	13 (82.4)	
Histological grade				
Well/moderate	65	37 (56.9)	28 (43.1)	0.092
Poor	35	13 (37.1)	22 (62.9)	
Tumor size				
<2 cm	56	37 (66.1)	19 (39.9)	<0.001
≥2 cm	46	13 (28.3)	33 (71.7)	
Lymph node invasion				
No	55	35 (63.6)	20 (36.4)	<0.05
Yes	45	15 (33.3)	30 (66.7)	
HER2				
Negative	73	42 (57.5)	31 (42.5)	<0.01
Positive	29	8 (27.6)	21 (72.4)	
ER				
Negative	31	11 (35.5)	20 (64.5)	0.086
Positive	71	39 (54.9)	32 (45.1)	
PR				
Negative	60	24 (40.0)	36 (60.0)	<0.05
Positive	42	26 (61.9)	16 (38.1)	

Abbreviations: ER, estrogen receptor; HER2, human epidermal growth factor receptor type2; PR, progesterone receptor.

inhibition of miR-1260b expression compared with transfection with miR-NC ($p < 0.01$, and $p < 0.01$, respectively) (Figure 2C). The miR-1260b inhibitor also induced a decrease in cell viability in dose- and time-dependent manner (Figure S2).

To further investigate whether miR-1260b affects migration and invasion, wound-healing and transwell invasion assays were performed. MDA-MB-231 cells transfected with the miR-1260b inhibitor showed lower migration potential compared with those transfected with miR-NC, and the cells transfected with the miR-1260b mimic showed higher migration potential under identical conditions (Figure 2D,E). In the transwell assay, the invasion ability of the cells treated with the miR-1260b mimic significantly increased compared with that of cells treated with miR-NC, and the ability of the cells treated with the miR-1260b inhibitor markedly decreased ($p < 0.01$, and $p < 0.01$, respectively) (Figure 2F).

3.3 | Effect of miR-1260b on apoptosis by directly targeting CASP8

To gain insight into the molecular mechanisms and to identify potential target genes of miR-1260b, RNA sequence analysis was

performed using total RNA extracted from MDA-MB-231 cells treated with the miR-1260b inhibitor and miR-NC. The selection criteria for the differentially expressed genes (DEGs) were as follows: log2 fold change ≥ 1.5 , p -value < 0.05 , and false discovery rate (FDR) < 0.05 . The heatmap profiles of differentially regulated transcripts are shown in Figure 3A. Among the 222 gene entities, 112 genes were upregulated directly or indirectly by miR-1260b inhibitor treatment (Figure 3B). Among the 112 upregulated genes, gene ontology (GO) analysis revealed that miR-1260b affects the regulation of transcription, proteasomal ubiquitin-dependent protein catabolic process, p53 class mediator, execution phase of apoptosis, and I-kappa B kinase/NF-kappa B signaling (Figure 3C). The top network contained mainly genes involved in the p53 pathway such as *ATF3*, *DUSP1*, and *KLFA* and apoptosis such as *GADD45B*, *GADD45A*, and *CASP8*; the key common gene was determined to be *CASP8* (Figure 3D). Of these candidate gene sets, potential target genes including *CASP8* were cross-examined using the software TargetScan 7.2 (Table S5). The relationship between miR-1260b and *CASP8* was verified by RT-qPCR. *CASP8* expression significantly increased in MDA-MB-231 cells treated with the miR-1260b inhibitor compared with those treated with miR-NC (Figure 3E). To further confirm the target relationship, both miR-1260b expression and

TABLE 2 Univariate and multivariate analysis of prognostic factors in breast cancer patients

Features	Univariate analysis			Multivariate analysis		
	HR	95% CI	p Value	HR	95% CI	p Value
Age (years)						
<50 vs. ≥50	0.804	0.279–2.318	0.687			
TNM stage						
Early stage vs. locally advanced stage	9.020	3.009–27.039	<0.001	6.053	1.935–18.932	<0.01
Histological grade						
Well/moderate vs poor	0.848	0.891–2.893	0.848			
Tumor size (cm)						
<2 vs ≥2	5.622	1.567–20.169	<0.01	5.723	1.593–20.557	<0.01
Lymph node invasion						
No vs yes	4.281	1.342–13.658	<0.05	3.599	1.067–12.134	<0.05
HER2						
Negative vs positive	4.714	1.635–13.598	<0.05	3.766	1.230–11.528	<0.01
ER						
Negative vs positive	0.350	0.123–0.998	<0.05	0.315	0.104–0.955	<0.05
PR						
Negative vs Positive	0.449	0.141–1.431	0.176			
miR-1260b expression						
Low vs high	8.523	1.906–38.109	<0.01	5.112	1.080–24.197	<0.05

Abbreviations: ER, estrogen receptor; HER2, human epidermal growth factor receptor type2; HR, hazard ratio; PR, progesterone receptor.

CASP8 expression in FFPE breast tissues ($n = 74$) were analyzed. There was a significant inverse relationship between the expression levels of miR-1260b and CASP8 (Spearman's rank correlation coefficient (r) of -0.6137 , $p < 0.0001$; Figure 3F).

To investigate whether the 3-UTR of CASP8 is a direct target of miR-1260b, dual-luciferase reporter assays were conducted (Figure 3G). Cotransfection of the MDA-MB-231 cells with WT CASP8 3-UTR/pmirGLO and the miR-1260b mimic caused a significant decrease in luciferase activity compared with that in cells transfected with miR-NC ($p = 0.008$). However, the luciferase activity of mutant CASP8 3-UTR/pmirGLO did not change after cotransfection with the miR-1260b mimic (Figure 3H). Additionally, Western blot analysis showed that the expression of caspase-8 and cleaved caspase-8 decreased in cells transfected with the miR-1260b mimic (Figure 3I).

Additionally, CASP8 was cross-validated in TCGA data using survival analysis. The results showed that patients with low CASP8 expression had poor survival outcomes (HR = 1.37 for total patients, HR = 1.75 for luminal A, HR = 1.75 for luminal B, HR = 1.45 for HER2, and HR = 1.96 for TNBC), which showed the opposite aspect to the survival curve according to miR-1260b expression (Figure S3).

3.4 | Regulation of intrinsic or extrinsic pathway of apoptosis by miR-1260b

In clinical settings, apoptosis is a key factor in the prediction of chemoresistance. As the earlier observed cell viability and

molecular features of miR-1260b were found to be related to apoptosis (Figure 3), we further sought to identify the association between miR-1260b and cell apoptosis. First, the rate of cellular apoptosis was analyzed using flow cytometry. MDA-MB-231 cells were treated with the miR-1260b inhibitor and miR-NC and incubated for 24 hours. The cells (1×10^5) were stained with annexin V-FITC and PI (Figure 4A). The rate of apoptosis in cells transfected with the miR-1260b inhibitor was significantly increased (21.15%) compared with that in cells transfected with miR-NC (7.27%) ($p < 0.001$) (Figure 4B).

To elucidate the mechanism of apoptosis after the inhibition of miR-1260b, the expression of apoptosis-related molecules was investigated by Western blot analysis. The cells treated with the miR-1260b inhibitor showed increased levels of cleaved poly adenosine diphosphate-ribose polymerase (PARP), cleaved caspase-3, and cleaved caspase-7 (Figure 4C). The activation of caspase-8 (extrinsic apoptosis) and caspase-9 (intrinsic apoptosis) was examined in cells treated with the miR-1260b inhibitor. Caspase-8 and -9 were cleaved in cells treated with the miR-1260b inhibitor (Figure 4C).

Subsequently, to further investigate the apoptotic pathway, the release of cytochrome *c* from mitochondria was investigated in cells treated with the miR-1260b inhibitor. MDA-MB-231 cells were treated with a miR-1260b inhibitor or miR-NC, and the cell lysates were separated into cytosolic and membrane fractions. Western blot analysis indicated that the inhibition of miR-1260b upregulated the translocation of cytochrome *c* from the

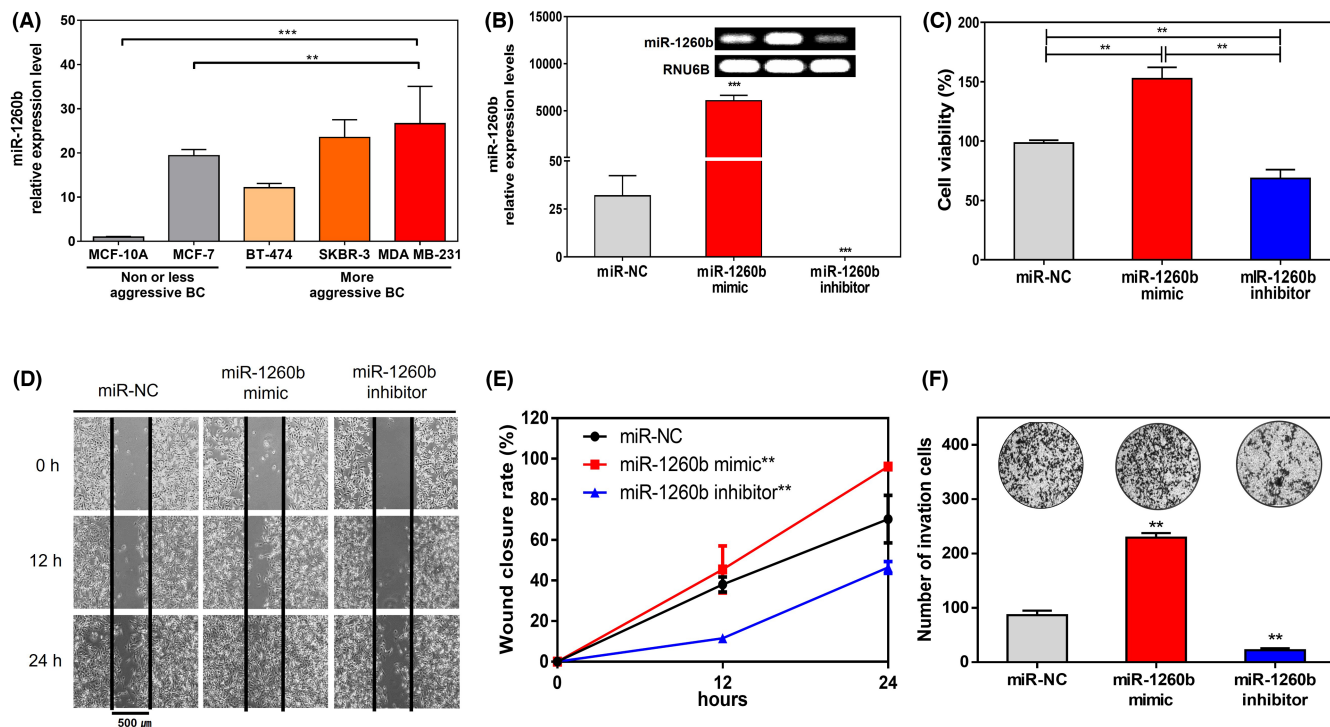


FIGURE 2 Graphs and images illustrating the effect of miR-1260b on cell viability, migration, and invasion of cancer cells. A, The relative expression level of miR-1260b in a normal breast cell line (MCF-10A) and four breast cancer cell lines (BT-474, and MCF-7, SKBR-3, and MDA MB-231). B, Promotion or inhibition of miR-1260b in MDA-MB-231 was confirmed by RT-qPCR and gel electrophoresis after treatment with miR-negative control (NC), the miR-1260b mimic, and the miR-1260b inhibitor. C, Cell viability was determined using water-soluble tetrazolium salt (WST) assay after treatment with miR-NC, the miR-1260b mimic, and the miR-1260b inhibitor. D, E, Migration analysis was performed using the wound-healing assay. Wound-healing closure changes were observed at 12 and 24 h. F, Cell invasion ability was analyzed using the transwell assay. The number of invading cells was measured by counting the number of cells that invaded through the membrane per field. The data are reported as the mean \pm standard deviation (SD). * $p < 0.05$, ** $p < 0.01$, *** $p < 0.001$

mitochondria to the cytosol (Figure 4D). The expression of XIAP and survivin was analyzed as an upstream regulatory molecule. It was found that survivin levels decreased, although the XIAP levels did not change in MDA-MB 231 cells treated with the miR-1260b inhibitor (Figure 4E).

3.5 | Role of miR-1260b as a useful biomarker for monitoring breast cancer

miRNAs are either encapsulated by exosomes or they circulate as free miRNAs and influence the adjacent cells/tissues.^{21,22} Therefore, we hypothesized that miR-1260b is possibly released from the cancer tissues into blood circulation. As a proof-of-concept for liquid biopsy-based assessments, the miR-1260b expression levels in plasma from 71 patients with breast cancer and 58 healthy controls were measured using RT-qPCR (Table S2). The expression levels of miR-1260b in patients with breast cancer (before treatment, $n = 54$) were significantly higher than those in healthy controls ($p < 0.001$) (Figure 5A). Subsequently, the miR-1260b expression was investigated by breast cancer subtypes and stages. The miR-1260b expression was significantly high in all subtypes, especially in the luminal B and HER2 subtypes ($p < 0.001$ in all subtypes vs healthy control)

(Figure 5B). miR-1260b expression in the plasma was higher in the early and locally advanced stages compared with that in the healthy control ($p < 0.001$ and $p = 0.0057$, respectively) (Figure 5C).

The diagnostic performance and cutoff value of miR-1260b were determined by receiver-operating characteristic (ROC) curve analysis. The area under the ROC curve (AUC) of miR-1260b was 0.90 (95% CI = 0.84–0.96, $p < 0.001$), and the cutoff point was 0.12 (Figure 5D). At the cutoff value, positive miR-1260b levels in the early-stage and locally advanced breast cancer before chemotherapy showed a 16.3-fold and 18.2-fold higher risk than the negative miR-1260b in each stage, respectively (Figure 5E). The positive miR-1260b level after neoadjuvant chemotherapy decreased the risk by 6.2%-fold.

4 | DISCUSSION

The tumorigenesis of miR-1260b in breast cancer cells was first reported in terms of proliferation, apoptosis, and migration. The novel target *CASP8* of miR-1260b was identified and validated in this study. Additionally, this study included the prognostic and diagnostic value of miR-1260b in breast cancer to investigate its potential utility in screening and diagnosis.

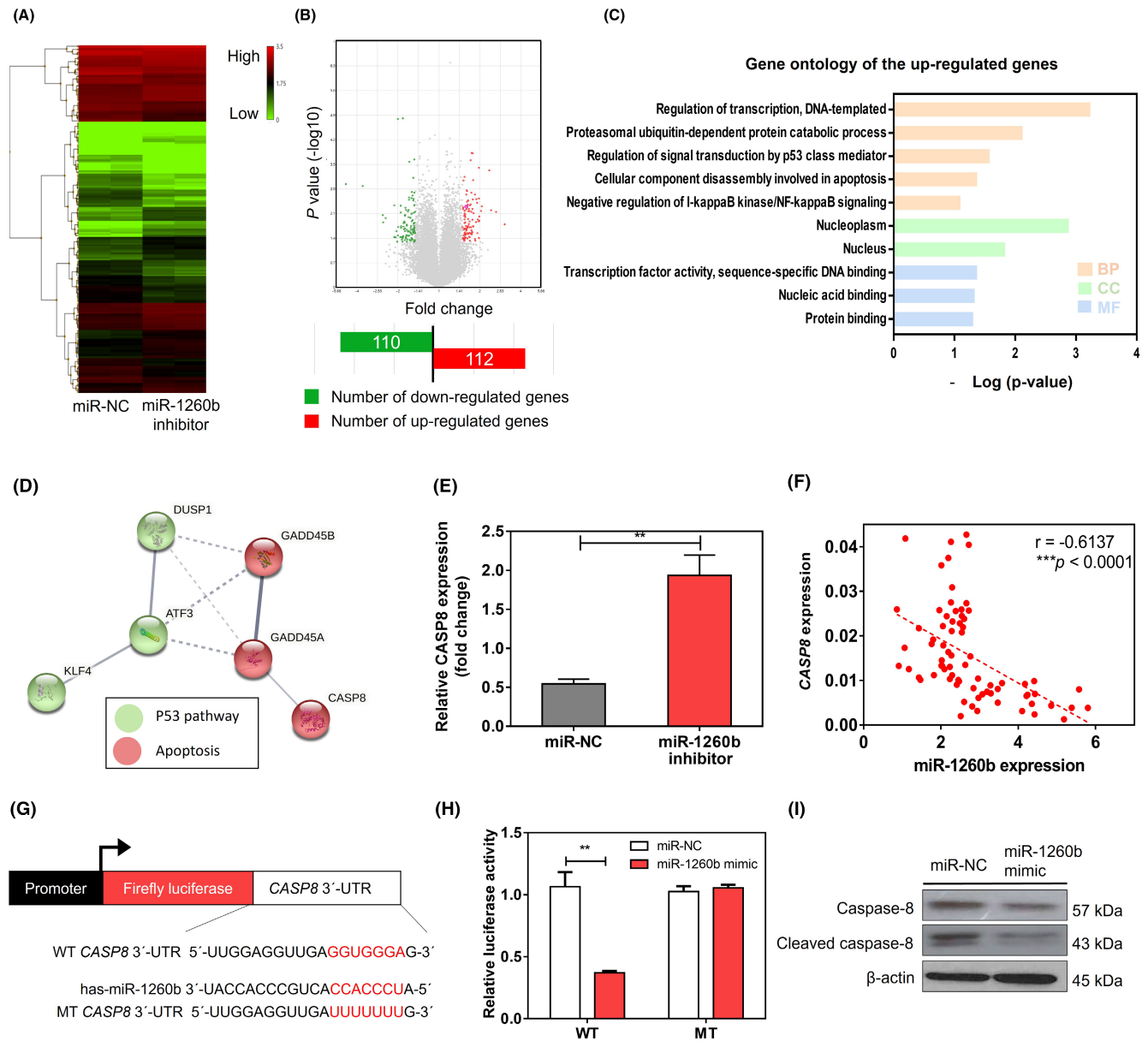


FIGURE 3 Prediction and validation of target genes for miR-1260b. Transcriptomic analysis of MDA-MB-231 cells treated with miR-negative control (NC) and those treated with the miR-1260b inhibitor. A, Heat map of the two-way hierarchical clustering (fold change 1.5, $p < 0.05$ and false discovery rate [FDR] < 0.05). The color scheme is based on the gene expression fold changes, with upregulation indicated with red color and downregulation with green color. B, Scatter plot depicting differentially expressed genes were identified upon miR-1260b inhibitor treatment as compared with the miR-NC. C, Graphical representation of gene ontology (GO) analysis for potential target genes of miR-1260b. Biological processes, cellular components, and molecular functions of GO were analyzed. D, Schematic of the search tool for retrieval of interacting genes (STRING) analysis for potential target gene of miR-1260b. E, Plots of the effects of the miR-1260b inhibitor on the mRNA expression levels of CASP8 in MDA-MB-231 cells. F, Scatter plot depicting the correlation between miR-1260b and CASP8 expression in breast cancer tissues ($r = -0.6137$, $p < 0.0001$, $n = 74$). G, H, Illustration and plot of the relative luciferase activities of plasmids carrying wild-type or mutant CASP8 3'-UTR in MDA-MB-231 cells cotransfected with the miR-1260b mimic. I, Image showing the protein expression of caspase-8 and cleaved caspase-8 in MDA-MB-231 overexpressing miR-1260b. The data are reported as the mean \pm standard deviation (SD). * $p < 0.05$, ** $p < 0.01$, *** $p < 0.001$

In clinical validation, the high expression of miR-1260b was more closely related to TNM stage, tumor size, and lymph node invasion. Despite significant advances in the early diagnosis and treatment of breast cancer, such as chemotherapy, radiotherapy, and surgery, the morbidity and mortality rates of advanced and metastatic breast cancer are approximately 50%.^{23,24} In our data, the Kaplan-Meier

analysis demonstrated that breast cancer patients in the high-miR-1260b-expression group had a significantly shorter OS than those in the low-miR-1260b-expression group. Cox regression analysis showed that high miR-1260b expression was an independent prognostic factor for poor survival. As miR-1260b is a potential predictor of poor prognosis through clinical evaluation, miR-1260b as a

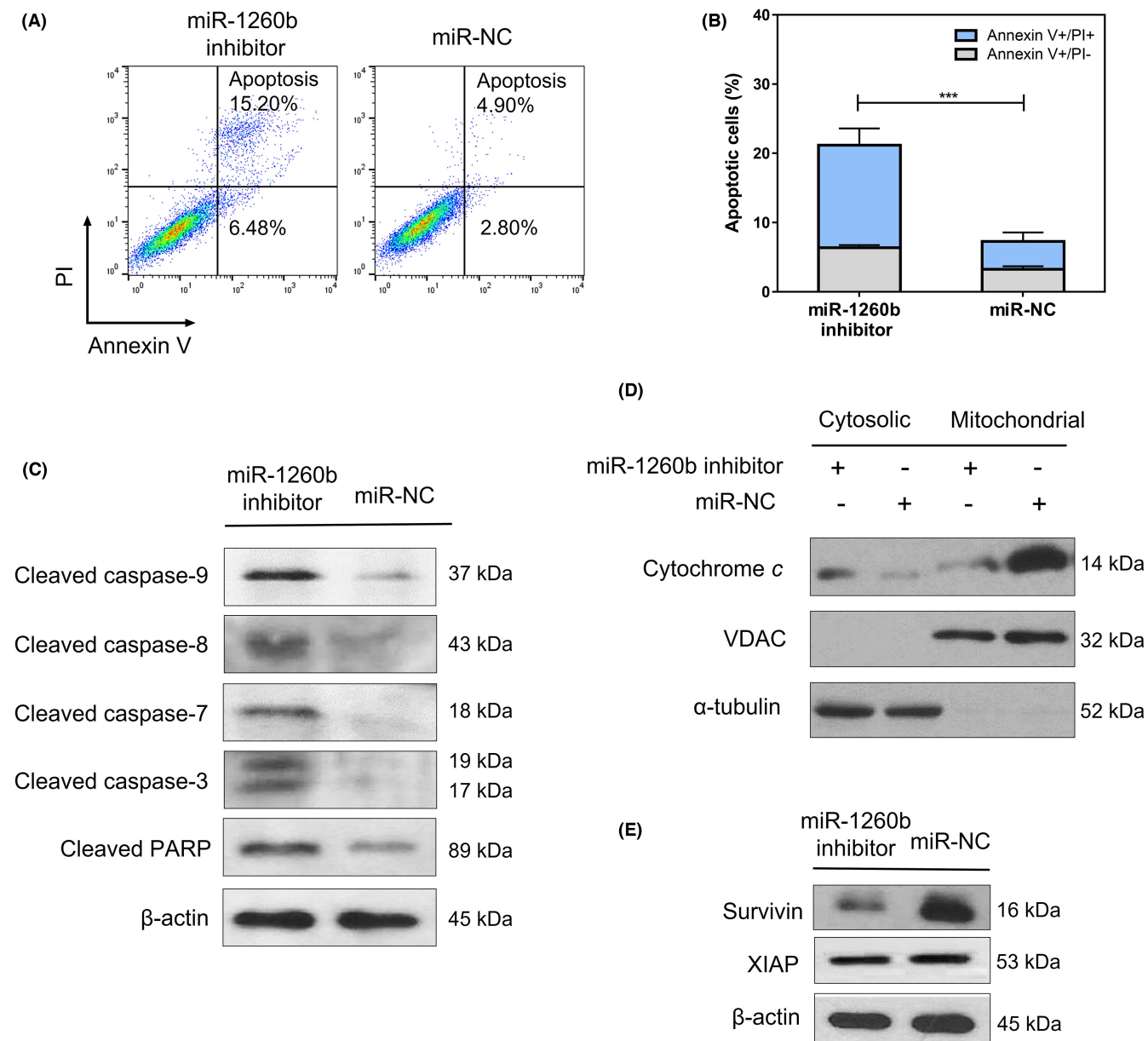


FIGURE 4 Inhibitory effects of miR-1260b on cell apoptosis. A, Plot showing the apoptotic cell population analyzed by flow cytometry. B, Percentages of apoptotic cells (early and late apoptosis rates) are indicated as a graph. C-E, Expression of active cleaved apoptotic proteins (C), cytochrome c (D), and antiapoptotic proteins (E) examined by Western blotting. β -actin was used as an internal control. VDAC and α -tubulin were used as markers of the mitochondrial and cytosolic fractions, respectively. The data are reported as the mean \pm standard deviation (SD). * $p < 0.05$, ** $p < 0.01$, *** $p < 0.001$

potential prognostic marker can be expanded in other types of metastatic cancers.

Our study also evaluated the potential clinical application of circulating miR-1260b in the diagnosis of breast cancer. The value of AUC was 0.90 (95% CI = 0.84-0.96, $p < 0.001$). Schwarzenbach et al. explored the diagnostic potential of a panel of circulating miRNAs targeting Phosphatase and Tensin Homolog deleted on Chromosome 10 (PTEN) tumor suppressors using RT-qPCR in 102 patients with breast cancer. The levels of circulating miR-20a and miR-21 were higher in cancer patients than in healthy controls. Additionally, the levels of circulating miR-214 can help differentiate between breast cancer and benign

and healthy controls with an AUC of 0.87 in ROC analysis.²⁵ Wang et al. showed that circulating miR-182 levels were significantly higher in patients with breast cancer than in healthy controls.²⁶ Similarly, Freres et al. also investigated the plasma miRNA profile determined by RT-qPCR in 108 patients with primary breast cancer. Receiver-operating characteristic curve from eight circulating miRNAs (miR-15, let-7d, miR-103, miR-107, miR-148a, let-7i, miR-19b, and miR-22*) exhibited an AUC of 0.81.²⁷ The diagnostic value of circulating miR-1260b is comparable to that of other circulating miRNAs in breast cancer.

Avoiding apoptosis is crucial for promoting tumorigenesis.²⁸ It helps cells avoid immune surveillance and survive in low-nutrient and

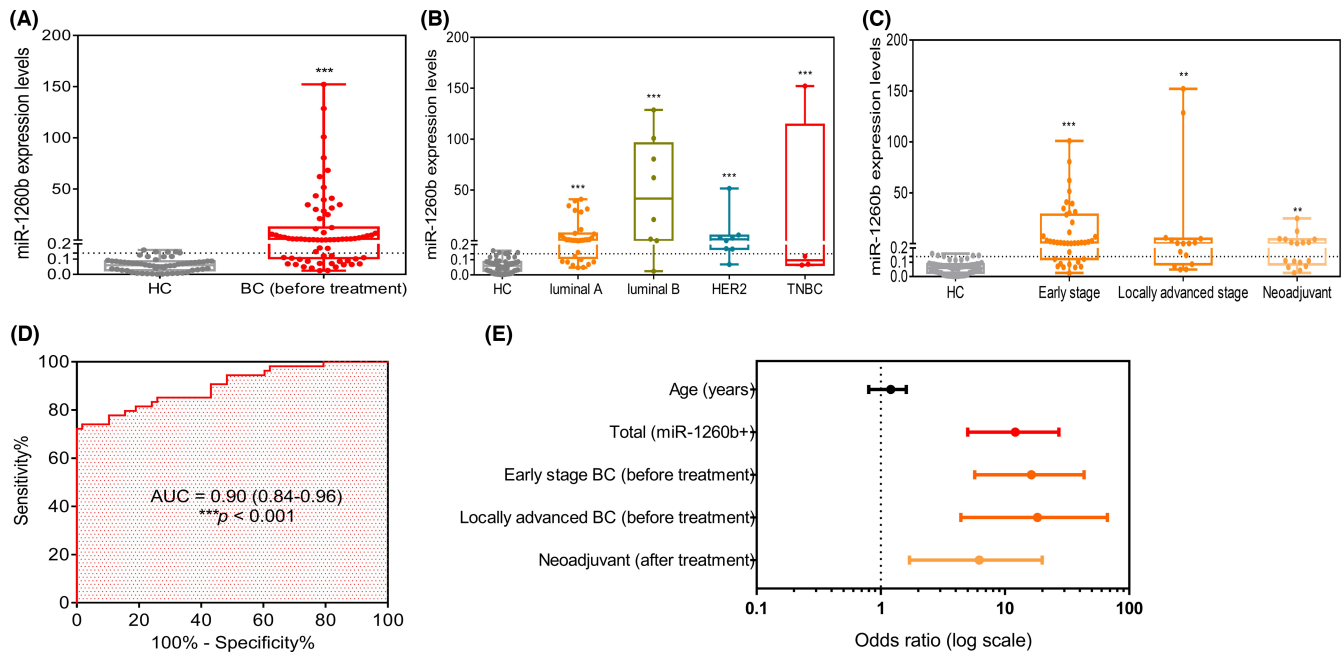


FIGURE 5 Plots depicting the clinical value of miR-1260b in plasma of breast cancer. A, miR-1260b expression level in plasma of patients with breast cancer and healthy controls. B, miR-1260b expression level in the plasma of healthy controls and patients, by breast cancer subtypes. C, miR-1260b expression level in the plasma of healthy controls and patients, by cancer stages. D, Receiver-operating characteristic curve (ROC) analysis result for the determination of the cutoff value to distinguish healthy controls and patients with breast cancer. E, Odds ratios of miR-1260b in the plasma of healthy controls and patients according to early breast cancer, locally advanced breast cancer, and neoadjuvant breast cancer. The data are reported as the mean \pm standard deviation (SD). Odds ratio is reported as median (95% CI) * $p < 0.05$, ** $p < 0.01$, *** $p < 0.001$

hypoxic tumor environments.²⁹ Caspase-9 and -8 are key molecules in the intrinsic and extrinsic apoptotic pathways, respectively.³⁰ In this study, cleavage of caspase-9, caspase-8, and PARP were found to increase when miR-1260b expression was inhibited. The main events of the intrinsic apoptotic pathway occur in the mitochondria including cytochrome *c* release, ROS production, and the involvement of apoptosis-regulating factors.³¹ Cytochrome *c* is a component of the electron transport chain in the mitochondria.³² One of the ways cell apoptosis is activated is by release of cytochrome *c* from the mitochondria into cytosol. The release of cytochrome *c* activates caspase 9.³³ We also found that the inhibition of miR-1260b upregulated the translocation of cytochrome *c* from the mitochondria to the cytosol, which suggested that miR-1260b can suppress apoptosis in breast cancer cells. Therefore, the upregulation of miR-1260b may facilitate the survival and development of breast cancer.

As miRNAs regulate the expression of target genes to exert their effects, identification of key target genes is crucial. Based on RNA sequence analysis and the TargetScan computer algorithm, 36 potential target genes of miR-1260b were identified. Among the 36 potential target genes, *CASP8*, which encodes caspase-8, was further investigated to confirm the direct target gene of miR-1260b. Analysis of breast FFPE tissue samples revealed an inverse relationship between miR-1260b and *CASP8* expressions. Further testing with luciferase assays indicated that *CASP8* was the target gene, which was directly regulated by miR-1260b. Variants of the *CASP8* gene are associated with breast cancer risk.³⁴⁻³⁶ *CASP8* knockdown increases

both the migratory and metastatic capacity of MDA-MB-231 and inhibits cell apoptosis.³⁷⁻³⁹ Therefore, *CASP8* is critically involved in regulating tumorigenesis. Several studies reported that miRNAs target the regulation of caspase-8 expression. Jin et al.⁴⁰ found that miR-24 and miR-221 modulate TNF-related apoptosis, which induces ligand resistance in hepatocellular carcinoma cells through caspase-8 and -3. Furthermore, Wang et al. showed that miR-874 regulates myocardial necrosis by targeting caspase-8.⁴¹ To the best of our knowledge, this is the first study to identify *CASP8* as a novel target of miR-1260b in breast cancer.

Several limitations should be considered when interpreting the findings of this study. First, all breast cancer patients in the present study were selected from a single hospital with small sample sizes. miR-1260b should be further investigated in a larger number of patients at various stages and subtypes from multiple centers. Further in vitro and in vivo investigations using various cancer cell lines, for studying the association between miR-1260b levels and driver gene mutations and performing miR-1260b target gene validation are necessary.

Conclusively, the present study suggests that miR-1260b can serve as a novel biomarker for the diagnosis and prognosis of breast cancer, as well as a potential therapeutic target.

ACKNOWLEDGMENTS

We are grateful to the Basic Science Research Program through the National Research Foundation of Korea (NRF) funded by the Ministry

of Science, ICT, and Future Planning (NRF-2020R11A1A01067448) for supporting this study through their grant.

DISCLOSURE

The authors declare no conflict of interest.

ORCID

Seung Il Kim  <https://orcid.org/0000-0001-9673-2748>

REFERENCES

- Mb A, Vs R, Me J, Ao A. Breast cancer biomarkers: risk assessment, diagnosis, prognosis, prediction of treatment efficacy and toxicity, and recurrence. *Curr Pharm Des*. 2014;20:4879-4898.
- WHO. Latest Global Cancer Data. Available online: <https://www.who.int/cancer/prevention/diagnosis-screening/breastcancer/en/>; 2018.
- Dillekas H, Rogers MS, Straume O. Are 90% of deaths from cancer caused by metastases? *Cancer Med*. 2019;8:5574-5576.
- Duffy MJ. CA 15-3 and related mucins as circulating markers in breast cancer. *Ann Clin Biochem*. 1999;36(Pt 5):579-586.
- Arslan N, Serdar M, Deveci S, et al. Use of CA15-3, CEA and prolactin for the primary diagnosis of breast cancer and correlation with the prognostic factors at the time of initial diagnosis. *Ann Nucl Med*. 2000;14:395-399.
- Harris L, Fritsche H, Mennel R, et al. American society of clinical oncology 2007 update of recommendations for the use of tumor markers in breast cancer. *J Clin Oncol*. 2007;25:5287-5312.
- Ng EK, Li R, Shin VY, Siu JM, Ma ES, Kwong A. MicroRNA-143 is downregulated in breast cancer and regulates DNA methyltransferases 3A in breast cancer cells. *Tumour Biol*. 2014;35:2591-2598.
- Nam SE, Lim W, Jeong J, et al. The prognostic significance of preoperative tumor marker (CEA, CA15-3) elevation in breast cancer patients: data from the Korean Breast Cancer Society Registry. *Breast Cancer Res Treat*. 2019;177:669-678.
- Rashed R, Darwish H, Omran M, Belal A, Zahran F. A novel serum metabolome score for breast cancer diagnosis. *Br J Biomed Sci*. 2020;77:196-201.
- Achkar NP, Cambiagno DA, Manavella PA. miRNA biogenesis: a dynamic pathway. *Trends Plant Sci*. 2016;21:1034-1044.
- Kozomara A, Griffiths-Jones S. miRBase: annotating high confidence microRNAs using deep sequencing data. *Nucleic Acids Res*. 2014;42:D68-D73.
- Kasinski AL, Slack FJ. Epigenetics and genetics. MicroRNAs en route to the clinic: progress in validating and targeting microRNAs for cancer therapy. *Nat Rev Cancer*. 2011;11:849-864.
- Stahlhut C, Slack FJ. MicroRNAs and the cancer phenotype: profiling, signatures and clinical implications. *Genome Med*. 2013;5:111.
- Hirata H, Ueno K, Nakajima K, et al. Genistein downregulates onco-miR-1260b and inhibits Wnt-signalling in renal cancer cells. *Br J Cancer*. 2013;108:2070-2078.
- Liu DR, Guan QL, Gao MT, Jiang L, Kang HX. miR-1260b is a potential prognostic biomarker in colorectal cancer. *Med Sci Monit*. 2016;22:2417-2423.
- Hirata H, Hinoda Y, Shahryari V, et al. Genistein downregulates onco-miR-1260b and upregulates sFRP1 and Smad4 via demethylation and histone modification in prostate cancer cells. *Br J Cancer*. 2014;110:1645-1654.
- Xu L, Xu X, Huang H, et al. MiR-1260b promotes the migration and invasion in non-small cell lung cancer via targeting PTPRK. *Pathol Res Pract*. 2018;214:776-783.
- Melo S, Sugimoto H, O'Connell J, et al. Cancer exosomes perform cell-independent microRNA biogenesis and promote tumorigenesis. *Cancer Cell*. 2014;26:707-721.
- Livak KJ, Schmittgen TD. Analysis of relative gene expression data using real-time quantitative PCR and the 2(-Delta Delta C(T)) method. *Methods*. 2001;25:402-408.
- Pfaffl MW, Horgan GW, Dempfle L. Relative expression software tool (REST) for group-wise comparison and statistical analysis of relative expression results in real-time PCR. *Nucleic Acids Res*. 2002;30:e36.
- Mitchell PS, Parkin RK, Kroh EM, et al. Circulating microRNAs as stable blood-based markers for cancer detection. *Proc Natl Acad Sci USA*. 2008;105:10513-10518.
- Kim MW, Park S, Lee H, et al. Multi-miRNA panel of tumor-derived extracellular vesicles as promising diagnostic biomarkers of early-stage breast cancer. *Cancer Sci*. 2021;112:5078-5087.
- Jemal A, Center MM, DeSantis C, Ward EM. Global patterns of cancer incidence and mortality rates and trends. *Cancer Epidemiol Biomarkers Prev*. 2010;19:1893-1907.
- Liu RZ, Garcia E, Glubrecht DD, Poon HY, Mackey JR, Godbout R. CRABP1 is associated with a poor prognosis in breast cancer: adding to the complexity of breast cancer cell response to retinoic acid. *Mol Cancer*. 2015;14:129.
- Schwarzenbach H, Milde-Langosch K, Steinbach B, Muller V, Pantel K. Diagnostic potential of PTEN-targeting miR-214 in the blood of breast cancer patients. *Breast Cancer Res Treat*. 2012;134:933-941.
- Wang P-Y, Gong H-T, Li B-F, et al. Higher expression of circulating miR-182 as a novel biomarker for breast cancer. *Oncol Lett*. 2013;6:1681-1686.
- Frères P, Wenric S, Boukerroucha M, et al. Circulating microRNA-based screening tool for breast cancer. *Oncotarget*. 2016;7:5416-5428.
- Plati J, Bucur O, Khosravi-Far R. Apoptotic cell signaling in cancer progression and therapy. *Integr Biol*. 2011;3:279-296.
- Lowe SW, Lin AW. Apoptosis in cancer. *Carcinogenesis*. 2000;21:485-495.
- Elmore S. Apoptosis: a review of programmed cell death. *Toxicol Pathol*. 2007;35:495-516.
- Mignotte B, Vayssiere JL. Mitochondria and apoptosis. *Eur J Biochem*. 1998;252:1-15.
- Tafani M, Karpinich NO, Hurster KA, et al. Cytochrome c release upon Fas receptor activation depends on translocation of full-length bid and the induction of the mitochondrial permeability transition. *J Biol Chem*. 2002;277:10073-10082.
- Kroemer G, Dallaporta B, Resche-Rigon M. The mitochondrial death/life regulator in apoptosis and necrosis. *Annu Rev Physiol*. 1998;60:619-642.
- Camp NJ, Parry M, Knight S, et al. Fine-mapping CASP8 risk variants in breast cancer. *Cancer Epidemiol Biomarkers Prev*. 2012;21:176-181.
- Lin W-Y, Camp NJ, Ghossaini M, et al. Identification and characterization of novel associations in the CASP8/ALS2CR12 region on chromosome 2 with breast cancer risk. *Hum Mol Genet*. 2015;24:285-298.
- Shephard ND, Abo R, Rigas SH, et al. A breast cancer risk haplotype in the caspase-8 gene. *Cancer Res*. 2009;69:2724-2728.
- Cano-Gonzalez A, Mauro-Lizcano M, Iglesias-Serret D, Gil J, Lopez-Rivas A. Involvement of both caspase-8 and Noxa-activated pathways in endoplasmic reticulum stress-induced apoptosis in triple-negative breast tumor cells. *Cell Death Dis*. 2018;9:134.
- De Blasio A, Di Fiore R, Morreale M, et al. Unusual roles of caspase-8 in triple-negative breast cancer cell line MDA-MB-231. *Int J Oncol*. 2016;48:2339-2348.
- Zhang N, Wang X, Huo Q, et al. The oncogene metadherin modulates the apoptotic pathway based on the tumor necrosis factor superfamily member TRAIL (Tumor Necrosis Factor-related Apoptosis-inducing Ligand) in breast cancer. *J Biol Chem*. 2013;288:9396-9407.

40. Jin X, Cai L, Wang C, et al. CASC2/miR-24/miR-221 modulates the TRAIL resistance of hepatocellular carcinoma cell through caspase-8/caspase-3. *Cell Death Dis.* 2018;9:318.
41. Wang K, Liu F, Zhou L-Y, et al. miR-874 regulates myocardial necrosis by targeting caspase-8. *Cell Death Dis.* 2013;4:e709.

SUPPORTING INFORMATION

Additional supporting information may be found in the online version of the article at the publisher's website.

How to cite this article: Park S, Kim J, Cho Y, et al. Promotion of tumorigenesis by miR-1260b-targeting CASP8: Potential diagnostic and prognostic marker for breast cancer. *Cancer Sci.* 2022;113:2097-2108. doi:[10.1111/cas.15345](https://doi.org/10.1111/cas.15345)